

Prototype and Performance Evaluation of Refrigerant-Refrigerant Microchannel Heat Exchanger

Authors: Susumu Yoshimura* and Shinichi Wakamoto*

1. Introduction

We developed a refrigerant-refrigerant microchannel heat exchanger, in which microchannel tubes consisting of several fluid paths through which low-temperature fluid and high-temperature fluid flow are joined, for the purpose of reducing the size and improving the performance of heat exchangers. From the results of performance evaluation of a prototype, we confirmed that the promotion of mixing of gas and liquid in the header could control the performance deterioration caused by maldistribution of a gas and liquid two-phase refrigerant, which was a major technological challenge in this type of heat exchanger.

2. Specifications of the Prototype and Test Method

2.1 Specifications of the Prototype

Figure 1 shows the prototype. Flat single tubes consisting of paths for the flow of low-temperature and high-temperature fluids, produced by aluminum extrusion, having a width of 25 mm and a thickness of 2 mm, are joined together. Two ends of the respective tubes are connected to the headers with a resultant configuration that provides five parallel flow units of low-temperature and high-temperature fluids. A single tube consists of 12 round microchannels having a cross-section with a 1 mm bore. The joints between singles tubes and between a single tube and the header are brazed together. The header bore is 6 mm and the effective length for heat exchange is 600 mm.

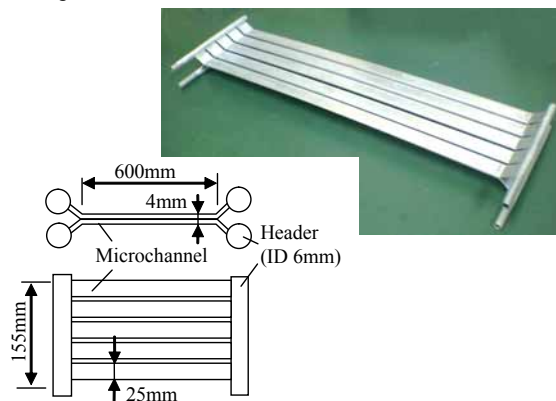


Fig. 1 Schematic view of the Prototype Heat Exchanger

2.2 Test conditions and test method

The operating fluids were R410A for cold fluid and water for hot fluid and these were counterflowed for heat exchange. Table 1 shows the test conditions. The cold fluid temperature T_{ci} and volume flow rate F of the hot fluid were fixed, while the hot fluid inlet temperature T_{hi} , mean mass velocity G of the cold fluid in the microchannel, and inlet quality X_i were changed. The header was positioned as shown in Fig. 2: (a) in a horizontal position and (b) in a vertical position. In a horizontal position, the heat exchanger was inclined at 50 degrees as shown in figure (a) and the fluid was introduced into the header horizontally and distributed downward vertically. On the other hand, in a vertical position, the fluid was introduced vertically and distributed horizontally. In the distribution section, the insertion δ of a single tube into the header was set at 0 and 2 mm. The inlet length on the low-temperature side through which two-phase fluid flow was 200 mm. The thermal conductance of the heat exchanger AK was determined from the measured values of the inlet and outlet temperatures T_{ci} and T_{co} of the cold fluid, inlet and outlet temperatures T_{hi} and T_{ho} of the hot fluid, and volume flow rate F , using equation (1) below. The C_p and $[LMTD]$ used in the equation are the specific heat at constant pressure and logarithmic mean temperature difference, respectively. The temperatures and flow rates mentioned below, unless otherwise specified, are those on the cold fluid side.

Table 1 Experimental conditions

G kg/m ² s	F L/min	T_{hi} °C	T_{ci} °C	X_i -
450 to 1300	2	37, 43	26.7	0.08 to 0.55

$$AK = \frac{\rho F C_p (T_{hi} - T_{ho})}{[LMTD]} \quad (1)$$

3. Results of the Test and Consideration

3.1 Single tube characteristics

First of all, to identify the characteristics without the influence of distribution, single tube characteristics were examined by removing one parallel flow unit from the

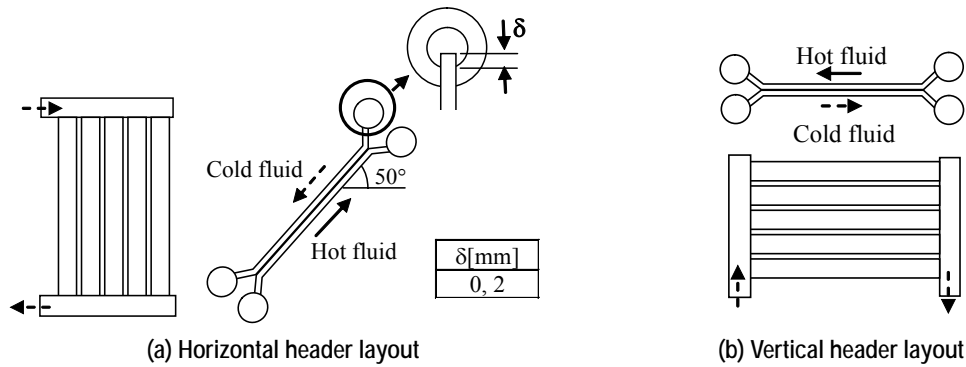


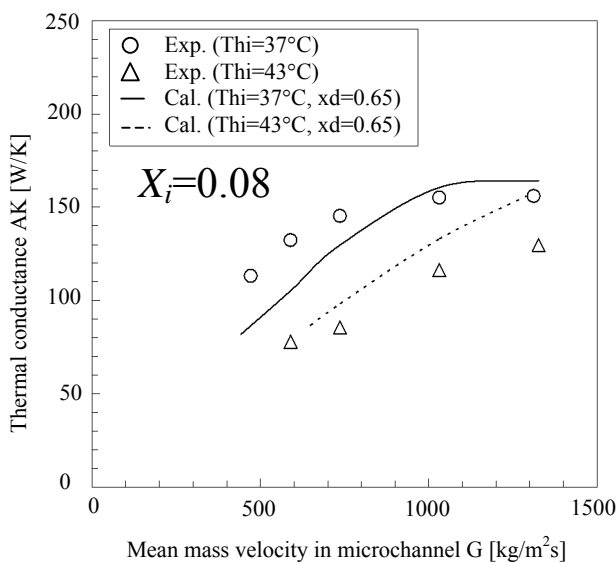
Fig. 2 Header layout and pipe insertion in the Prototype Heat Exchanger

prototype. The heat exchanger was set at an inclination of 50 degrees, as shown in the Fig. 2(a).

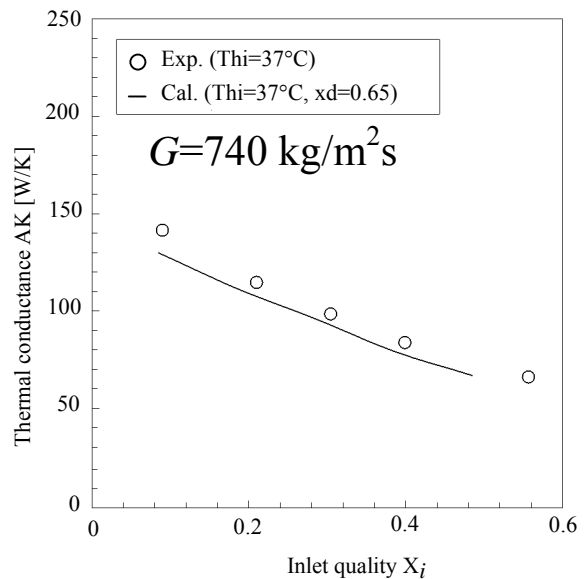
Figures 3(a) and 3(b) show the influence of the mean mass velocity G and inlet quality X_i in the microchannel on the thermal conductance AK , based on the results of the test. The marks \circ and \triangle in Fig. 3 indicate the hot fluid inlet temperature $T_{hi} = 37^\circ\text{C}$ and 43°C . AK increased with the mass velocity G and decreased with increasing inlet quality X_i . AK also decreased with an increasing hot fluid inlet temperature T_{hi} .

Thereafter, we compared the test results with the results of the calculation, using the heat transfer calculation model described below. For the heat transfer model, the heat exchanger (length: L) was divided into N elements in a longitudinal direction. Furthermore, as shown in Fig. 4, the heat exchanger was divided in the microchannel layout direction (number of channels: N_{ch} and pitch: p). The value of N was 30. The thermal con-

ductance AK_i (microchannel wetted surface area basis) of each divided element "i" consisted of heat transfer coefficients (heat transfer coefficients α_h and α_c) of the hot and cold fluids, thermal conductivity of the flat tube (thermal conductivity of material λ_t), and thermal contact conductance α_{cl} of the brazing layer. L_i is the length of an element. For thermal conduction of the flat tube, it was divided into the portion contacting the brazing-layer (portion A) and the portion between the centers of channel holes (portion B). Portion B was expressed by a fin having a wetted perimeter πD , an average thickness t_{av} , length D , thermal conductivity λ_t and efficiency ϕ . The applicability of the fin mentioned above to represent portion B reasonably was verified previously by a two-dimensional numerical calculation. "t" is the distance from the brazing layer to the microchannel. Dittus-Boelter's equation⁽¹⁾ was used for the heat transfer coefficient α_h of the hot fluid, while Yu et al.'s equation⁽²⁾ was used for the heat transfer coefficient α_c of the cold two-phase fluid. Furthermore, the dryout zone taken into the heat transfer coefficient α_c



(a) Relation between G and AK



(b) Relation between X_i and AK

Fig. 3 Thermal conductance with varying mean mass velocity and quality in the microchannel

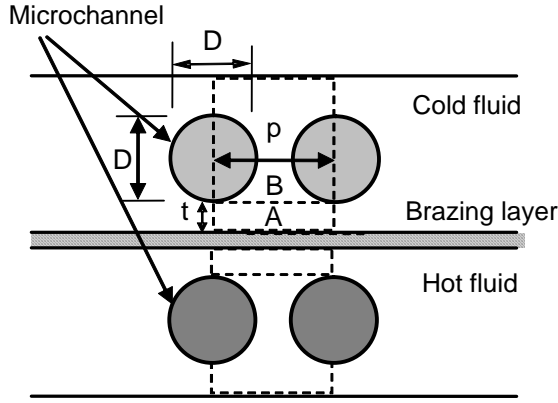


Fig. 4 Schematic view of the hat transfer model

was calculated by Dittus-Boelter's equation on the assumption that the heat transfer coefficient is that in gas single-phase flow at dryout quality X_d or higher. For the value of X_d , the average 0.65 of the values, 0.6 to 0.7, reported in the study on the characteristics of evaporating heat transfer of microchannel tubes by Kuwahara et al.⁽²⁾ was used.

Calculations for AK are expressed by equations (2) through (5) below. The thermal contact conductance α_{cl} was obtained by first performing an experiment on water-to-water heat exchange, and next by determining the value of AK from equation (1), and then calculating equations (2) to (5), to finally obtain $\alpha_{cl} = 1.7 \times 10^5$ W/m²K. Since both the cold and hot fluids are a single-phase flow in this case, α_c was also determined by Dittus-Boelter's equation. The value of AK was thus calculated by using equation (2) from the heat transfer rate Q, which was the total sum of the heat transfer rate of the respective divided elements.

$$Q = AK[LMTD] = \sum_i^N AK_i[LMTD]_i \quad (2)$$

$$AK_i = \pi DN_{ch} L_i \left\{ \frac{1}{\phi_h \alpha_h} + \frac{2\pi D}{p} \frac{t}{\lambda_t} + \frac{\pi D}{p \alpha_{cl}} + \frac{1}{\phi_c \alpha_c} \right\}^{-1} \quad (3)$$

$$\phi = \frac{\tanh \left(\frac{(\pi D) \alpha}{\lambda_t t_{av}} \right)}{\sqrt{\frac{(\pi D) \alpha}{\lambda_t t_{av}}}} \quad (4)$$

$$t_{av} = p - \frac{\pi}{4} D \quad (5)$$

Figure 3 shows the results of the calculations: the solid line for $T_{hi} = 37^\circ\text{C}$ and the dotted line for $T_{hi} = 43^\circ\text{C}$. $T_{hi} = 37^\circ\text{C}$ and $T_{hi} = 43^\circ\text{C}$ correspond to the average heat flux of approximately 40 kW/m² and 50 kW/m². The trends in the calculated and experiment values largely agree. On the other hand, the difference between the calculated values and experiment values

could be attributed to the dryout quality X_d and the heat transfer models in the dryout zone.

3.2 Performance of the prototype

Figure 5(a) shows the relationship between the thermal conductance AK of the prototype and the mass velocity G_{hd} at the inlet header (horizontal axis), while Fig. 5(b) shows the relationship between the thermal conductance AK of the prototype and the inlet quality X_i (horizontal axis). The \circ marks in the figure indicate values that are five times the AK and G_{hd} , obtained on the basis of the single tube characteristics described in section 3.1 above. The AK of the prototype grew to be AK = 480 through 700 W/K at $X_i = 0.08$ and $G_{hd} = 800$ to 1200 kg/m²s in the horizontal position and a pipe insertion at distribution section of $\delta = 2$ mm (marked with \bullet in the figure) and decreased to AK = 700 to 490 W/K for $X_i = 0.08$ to 0.3. The mean mass velocity G in the microchannel was G = 450 to 700 kg/m²s in the range of $G_{hd} = 800$ to 1200.

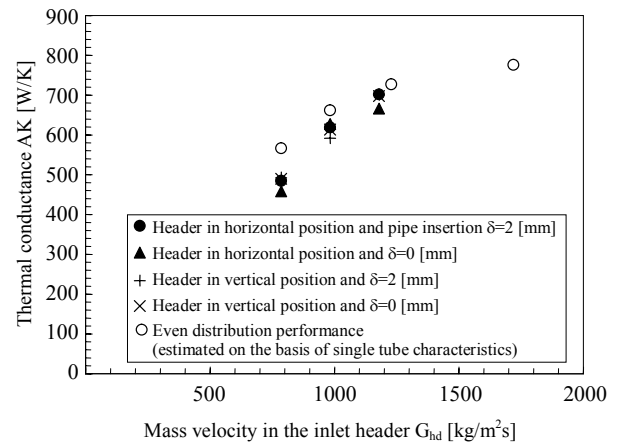
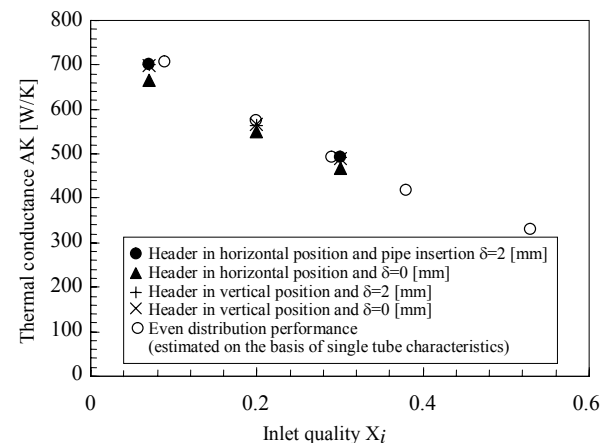

 (a) Relation between G and AK

 (b) Relation between X_i and AK

Fig. 5 Thermal conductance with varying mean mass velocity and quality in the microchannel

Compared with the single tube characteristics, performance deterioration assumed to be attributable to maldistribution was found to be 2 to 5% for $G_{hd} = 1000$

or higher, which was shown to be comparatively small. Regarding inlet quality X_i , the larger X_i was, the more the performance deterioration was reduced. The influence of the header position or the pipe insertion at the distribution section on performance, was confirmed to be limited.

The factor of the findings mentioned above can be explained as follows.

In Fig. 6, the horizontal axis shows the corrected gas mass velocity, calculated by dividing the mass velocity G_g of the refrigerant gas in the inlet header as expressed by equation (6) by parameter $\lambda^{(3)}$ in the Baker map, which is used as the flow regime map of the two-phase flow, while the vertical axis shows the ratio of the thermal conductance AK to AK during even distribution without maldistribution. (The value was obtained by dividing the data marked with ●, ▲, +, and × by the data marked with ○ in Fig. 5.)

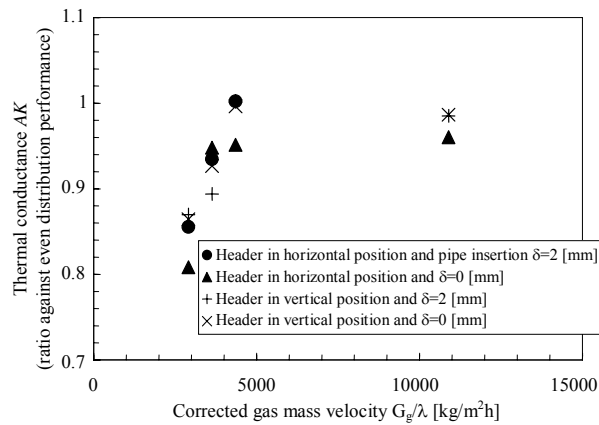


Fig. 6 Thermal conductance with varying corrected mass velocity in the header

$$G_g/\lambda = X_i G_{hd}/\lambda \tag{6}$$

AK increases with increasing G_g/λ to gradually approached 1. From this, it can be assumed that the reason why even distribution is advanced with increasing flow rate and inlet quality, and performance deterioration is consequently reduced, is that the gas velocity increases in the inlet header and the mixing of gas and liquid is increased in the flow.

The authors clearly identified the basic characteristics of the refrigerant-refrigerant microchannel heat exchanger. The authors are going to expand the range of conditions for evaluating the characteristics and continue the study to improve flow distribution.

References

- (1) F. W. Dittus, L.M.K. Boelter: Univ. Calif. Publ. Eng., 2, 433 (1930).
- (2) K. Kuwahara et al.: Trans. of JAR, 21(2), 121-128 (2004).
- (3) O. Baker: J. Oil & Gas, 53, 185 (1954).